

Does VLM Classification Benefit from LLM Description Semantics?

Pingchuan Ma*, Lennart Rietdorf*, Dmytro Kotovenko, Vincent Tao Hu, Björn Ommer

CompVis @ LMU Munich
Munich Center for Machine Learning (MCML)

Abstract

Accurately describing images via text is a foundation of explainable AI. Vision-Language Models (VLMs) like CLIP have recently addressed this by aligning images and texts in a shared embedding space, expressing semantic similarities between vision and language embeddings. VLM classification can be improved with descriptions generated by Large Language Models (LLMs). However, it is difficult to determine the contribution of actual description semantics, as the performance gain may also stem from a semantic-agnostic ensembling effect. Considering this, we ask how to distinguish the actual discriminative power of descriptions from performance boosts that potentially rely on an ensembling effect. To study this, we propose an alternative evaluation scenario that shows a characteristic behavior if the used descriptions have discriminative power. Furthermore, we propose a training-free method to select discriminative descriptions that work independently of classname ensembling effects. The training-free method works in the following way: A test image has a local CLIP label neighborhood, *i.e.*, its top- k label predictions. Then, w.r.t. to a small selection set, we extract descriptions that distinguish each class well in the local neighborhood. Using the selected descriptions, we demonstrate improved classification accuracy across seven datasets and provide in-depth analysis and insights into the explainability of description-based image classification by VLMs.

Code — <https://github.com/CompVis/DisCLIP>

1 Introduction

Human visual recognition is closely tied to verbal reasoning, as it often relies on the ability to express visual information in words (Zhao et al. 2022). However, a neural network usually does not exhibit this property, making its explainability a significant concern for the machine learning community. Some studies (Zhang et al. 2024; Hakimov and Schlangen 2023) aim to connect visual cues and textual descriptions, but these usually require extensive human subject analysis and highly specific datasets with annotations (Young et al. 2014), which are costly to obtain (Lin et al. 2014).

Vision-Language Models (VLM) (Radford et al. 2021; Li et al. 2021, 2019) tackle this issue by training neural networks to link images and their textual descriptions

*These authors contributed equally.

within a shared embedding space. This enhances the correlation between visual and textual details. VLMs can be applied to zero-shot image classification by passing an image through the VLM’s image encoder and prompting the text encoder with hand-crafted inputs like “*a photo of a [classname]*” (Radford et al. 2021). Recent work (Menon and Vondrick 2022) extends this approach by incorporating additional descriptions generated by Large Language Models (LLMs) for each class name. LLMs like GPT-3 (Brown et al. 2020; Ouyang et al. 2022) or Llama (Touvron et al. 2023), trained on extensive text corpora, are intended to provide richer semantics, enhancing VLM classification.

However, *Does VLM classification truly benefit from LLM-generated description semantics?* This work explores this core question as LLM-generated descriptions present several challenges. For example, descriptions can overlap for similar classes — such as parrots and sparrows — both described as having feathers, which is not a distinguishing feature. Moreover, while supplying the model with as many LLM-generated descriptions as possible may seem advantageous, it results in excessively lengthy collections. This complicates understanding the contribution of each description to the final decision.

Another problem is the structured noise ensembling phenomenon (Roth et al. 2023): LLM-generated descriptions can be replaced with random characters and high-level concepts (such as “*Baklava*”, “*a food that is 34mfqr5*”) while still improving the model performance. This raises the question of whether the improvement is due to additional semantics of the LLM-generated descriptions or to the ensemble effect of the noise augmentation.

Given these challenges, a proposed model should meet three criteria: 1) As humans who describe with a limited set of descriptions, the model should also operate with a manageable number of text descriptions. 2) These descriptions should be semantically meaningful. 3) The model should be resilient to noise ensembling. To address the issue of structured noise ensembling, we constrain the model to use only textual descriptions that do not contain the classname, *i.e.* classname-free descriptions.

Additionally, we employ a training-free algorithm that processes textual description embeddings within the neighborhood of the queried image embedding. This approach narrows the focus to descriptions relevant to distinguishing

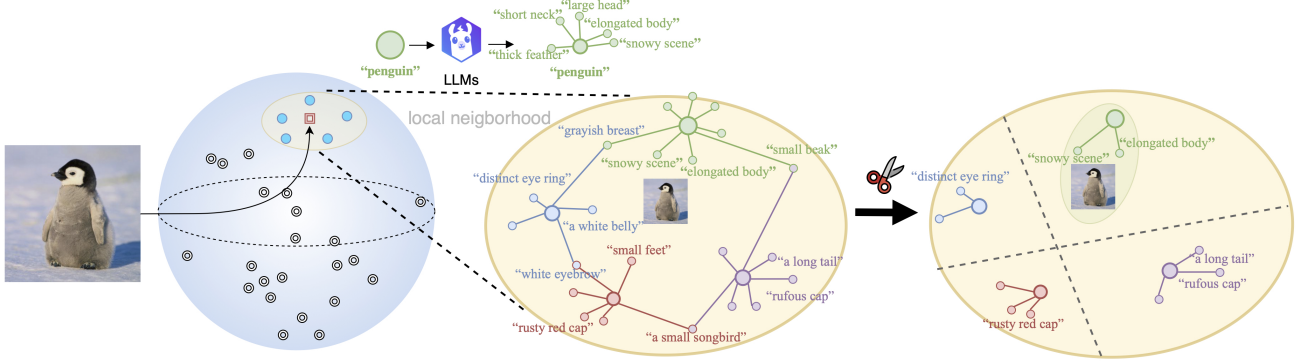


Figure 1: **Are the extra semantics provided by LLM truly useful?** Our method first identifies candidate labels using only the class name. We then filter out descriptions that may seem logical but do not differentiate the group, such as those ambiguous, overly generic, or act as noise. This refinement ensures that the remaining descriptions provide distinctive vision-language cues within the local candidate neighborhood, offering more specificity than the class name alone can capture.

between the specific subset of ambiguous classes, reducing the information to process and targeting a more manageable problem rather than attempting to differentiate across all classes. Our method passes the image through the CLIP image encoder, identifies a set of ambiguous class names representing possible candidates, and then applies a straightforward procedure to determine the most distinctive descriptions for these candidates, as shown in Figure 1.

Moreover, our method uses the text embedding of the class name only once and subsequently leverages class name-free LLM-generated descriptions. Therefore, we ensure that performance gains are not due to noisy augmentations of the class names but rather to a semantically meaningful enrichment. In summary, our contribution is threefold:

- We propose an alternative evaluation scenario for VLM classification tasks to assess whether performance gains stem from genuine semantic understanding rather than an ensemble effect, which is difficult to discern under conventional setups (Table 1 and Figure 3).
- Using this alternative setup, we introduce a training-free approach (Section 3.2) that narrows the focus to a small neighborhood and selects precise, semantically meaningful, and distinguishing class descriptions to improve the VLM classification performance (illustrated in Figure 1).
- Our method achieves improved performance compared to related approaches in two different setups, offering insight into the explainability of fine-grained image classification with VLMs (in Section 4.2).

2 Related Works

Vision-Language models for classification Vision-language models such as (Radford et al. 2021) can be used for classification. Notable training-free approaches that build on top of this include DCLIP (Menon and Vondrick 2022) and CuPL (Pratt et al. 2023), where class name texts are augmented with knowledge contained in LLMs to leverage seemingly discriminating characteristics to achieve

performance boosts. As (Roth et al. 2023) demonstrated, similar effects could be obtained by augmenting the class name with text noise and high-level concepts, raising concerns that many performance gains from DCLIP (Menon and Vondrick 2022) were not due to additional semantics but rather to introduced noise. FuDD (Esfandiarpour and Bach 2024) introduced contrastive zero-shot prompting to obtain a more diverse set of text prompts. The disadvantage of these approaches is that they rely on ensembling the description extended class name multiple times to achieve significant gains, making it difficult to separate additional semantics from random augmentations of the class name.

Notable approaches that train in the CLIP embedding space include (Yan et al. 2023), where nearest neighbors from a pool of text embeddings replace linear weights of a learned dictionary, and LaBo (Yang et al. 2023), which trained a linear classifier on a wide and global bottleneck of language activations selected for diversity and coverage. (Zhou et al. 2022) performed non-explainable tuning of text prompt embeddings to optimize classification, while (Zang et al. 2024) trained the last layer of image and text encoders over a concept bottleneck to discover explainable concepts. (Feng, Bair, and Kolter 2023) trained a sparse logistic regression over a matrix of image-language activations, with the training signal also used to train the image encoder.

In contrast to the methods outlined above, our approach delivers humanly understandable (thus explainable), semantically meaningful, disjoint, and distinguishing language descriptions in text space through a training-free method, which boosts VLMs classification accuracy while providing higher explainability. Reasons for this better explainability can be found in Section 3.2.

Test Time (noise) Augmentation Data augmentation involves increasing the diversity of training examples without explicitly collecting new data. It can also be employed at test time to enhance robustness (Cohen, Rosenfeld, and Kolter 2019) and improve accuracy (Szegedy et al. 2015; Jin et al. 2018). Notably, simply adding noise to the input string

at different levels (Kobayashi 2018; Şahin 2022; Belinkov and Bisk 2018) or their textual embeddings (Sun et al. 2020; Chen, Yang, and Yang 2020; Hao et al. 2023), can achieve similar effects on both performance and robustness across various tasks and domains (Feng et al. 2021).

Test Time Augmentation TTA introduces an *ensemble* of predictions from several transformed or distorted versions of a given test input to obtain a “smoothed” prediction. For example, one could average the predictions from various modified versions of a given string, ensuring that the final prediction is robust to any single unfavorable version (Roth et al. 2023; Menon and Vondrick 2022; Esfandiarpour and Bach 2024).

Some previous methods (Esfandiarpour and Bach 2024) used up to hundreds of thousands of descriptions per class, achieving significant improvements in classification accuracy with VLM. However, it is challenging to determine if the performance gains result from the vast ensemble or true information, hence hindering explainability.

3 Method

First, we introduce the conventional task formulation for image classification using Vision-Language Models. We then present our unique approach to this task to enable interpretability. Finally, we propose a specific solution to enhance the results further.

3.1 Background

VLM for Visual Classification The process of image classification by Vision-Language Models (VLMs) occurs as follows: Given an image x and a set of class labels \mathcal{C} , one classifies the image x by retrieving the class label \tilde{c} with the highest vision-language score:

$$\tilde{c} = \arg \max_{c \in \mathcal{C}} s(c, x), \quad (1)$$

where the vision-language scores $s(c, x)$ use a function $\phi(\cdot, \cdot)$, to calculate similarity scores for image-text embedding pairs. A typical instance of $\phi(\cdot, \cdot)$ is the usual cosine similarity. Traditionally, a vision-language score is obtained in the following way: using the image-text embedding function e of the VLM and given a text representation (a string containing the class name) t_c of class label c :

$$s(c, x) = \phi(e(t_c), e(x)), \quad (2)$$

where $e(\cdot)$ is the image or language embedding. Another way to obtain vision-language scores is via ensembling. The motivation for that ensembling is from how a human describes an object. For example, when describing an apple, we can describe it as a “green stuff”, “a round object”, or “fruit of the same size as an orange”. In this case, there is no single text representation t_c for a class c but a set of language representations $\mathcal{D}(c)$ where the ensembling happens over the elements of $\mathcal{D}(c)$:

$$s(c, x) = \frac{1}{|\mathcal{D}(c)|} \sum_{d \in \mathcal{D}(c)} \phi(e(d), e(x)), \quad (3)$$

In the course of this work and w.r.t. to textual descriptions, we call a set $\mathcal{D}(c)$ a description assignment. Furthermore, an LLM “assigns” descriptions by generating them when prompted for a particular class c , yielding the assignments $\mathcal{D}(c)$. The elements of $\mathcal{D}(c)$ can be pure text augmentations, e.g. “an image of [cls]”, “a photo of [cls]”, or can contain LLM-generated text descriptions and high-level-concepts, e.g. “an image of [cls], a type of [LLM-generated category], with [LLM-generated descriptions]”. Most of the approaches (Menon and Vondrick 2022; Pratt et al. 2023; Esfandiarpour and Bach 2024; Roth et al. 2023) that use ensembling as in Equation (3) with LLM-generated contents always include the class name token [cls] for $\forall d \in \mathcal{D}(c)$, which we denoted as *Classname-included descriptions*.

3.2 Our Approach

Classname-free descriptions In the conventional setup (Menon and Vondrick 2022; Pratt et al. 2023; Esfandiarpour and Bach 2024), performance gains may result from the noise augmentation of the class name text [cls] embedding through its various combinations with [LLM-generated category], [LLM-generated descriptions], and even random strings. While random strings should not contribute extra semantics and be embedded far away from [cls], this can sometimes apply to LLM-assigned text as well due to the vocabulary discrepancy between VLMs and LLMs. Another cause may also be the fact that the images do not exhibit the described property. Despite this, such combinations can still achieve good performance even though the assigned descriptions are not semantically correct.

To better investigate whether the improved performance stems from semantic enrichment or merely from the ensemble effect, we propose an approach where, out of all elements in $\mathcal{D}(c)$, exactly one element should contain the class name c . The remaining elements must contain textual descriptions without the class name. This set of descriptions then becomes:

$$\mathcal{D}(c) = \{d^{c+}, d_0^{c-}, \dots, d_m^{c-}\}, \quad (4)$$

where d^{c+} denotes that the description contains the class name, while d^{c-} denotes that it does not. A typical $\mathcal{D}(c)$ can therefore be the following: {“An image of apple pie.”, “crispy brown crust”, “graham cracker crust”}. Whereas in the conventional setup, the [cls] would be the following {“An image of apple pie.”, “An image of apple pie with crispy brown crust”, “An image of apple pie with graham cracker crust”}. The comparison of different setups is shown in Figure 2.

Different weight for `cls` As discussed previously, under the conventional scenario, the evaluation of the language-ensembling VLM method is a simple averaging of aggregated class-specific similarities between the image and descriptions. However, in our classname-free setup, it is unclear if plain averaging across the obtained classname-free

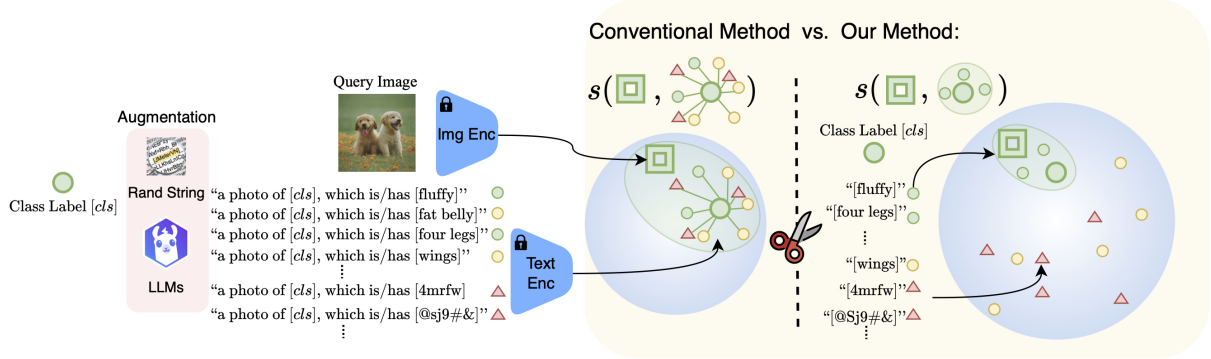


Figure 2: Our Method. In the conventional setup (*left*), using CLIP with LLM-generated class descriptions or random strings can sometimes result in performance gains due to the added semantics or the ensemble effect. However, when the classname is removed, *i.e.* under the proposed classname-free setup (*right*), these descriptions will fail to perform well, as only meaningful descriptions w.r.t. the class are useful where random strings or not informative descriptions bring no gain.

descriptions and the single cls is appropriate. This is because the classname is probably the most important text representation of the class, whereas the classname-free descriptions rather have a supporting, distinguishing character. To address this challenge in our evaluation, a weighting factor $w_{cls} \in \mathbb{R}^+$ gets introduced to the vision-language ensemble:

$$s(c, x) = \frac{1}{|\mathcal{D}(c)|} \sum_{d \in \mathcal{D}(c)} w(d) \cdot \phi(d, x) \quad (5)$$

with

$$w(d) = \begin{cases} w_{cls} & \text{if } d = d_{cls}, \\ \frac{1}{|\mathcal{D}(c)|-1} & \text{if } d \in \mathcal{D}(c) \setminus \{d_{cls}\}. \end{cases}$$

Weights of the classname-free descriptions are normalized to one in order to have the same relative weightings between classes with different amounts of assigned descriptions. Nonetheless, the challenge remains how to find class-specific, classname-free descriptions that actually boost the classification accuracy, which we will discuss next.

Selection of descriptions Our method works in a local candidate neighborhood: Given a test image x_i , one retrieves its top- k predictions based solely on text embeddings of texts such as “*a photo of [cls]*”. These preliminary candidate labels constitute the image’s local label neighborhood $\mathcal{A}(x_i) = \{a_0, a_1, \dots, a_k\}$, in which more fine-grained descriptions can offer further distinctiveness.

The image-language similarities of class descriptions can correlate positively or negatively with ambiguous candidateclassnames of a test image. Ideally, one wants to find descriptions that only correlate positively with one of the ambiguous classnames and negatively with all the others - hence providing a distinctive and explainable language representation. Consequently, the assignment of classname-free descriptions of classes denoted as $\mathcal{D}(c)$ can significantly influence the final classification result. For example, an albatross might be best distinguished from a penguin by “*sailing through the air*” while it might not be well told apart by “*is a*

seabird” since both classes share this feature. Furthermore, this connection must also be well represented in the VLM embedding space.

Algorithm 1 depicts our proposed procedure to find such descriptions. Having available n reference image samples per class c and a global, classname-free description pool \mathcal{P} to select from, the goal is to find a set of descriptions $\mathcal{D}(c) \subset \mathcal{P}$ with $|\mathcal{D}(c)| = m$ that distinguishes each class $a \in \mathcal{A}(x_i)$ from its most ambiguous classes $a' \in \mathcal{A}(x_i) \setminus a$, *i.e.* the small neighborhood of classes around the given images, as depicted in the left part of Figure 1. For that, one utilizes a lookup matrix S containing classwise averaged image-description similarities to obtain feedback from the VLM embedding space. The criterion for assigning descriptions $D(a)$ is a score that is positive if a description activates on average higher for $c = a$ than for all $a' \in \mathcal{A}(x_i) \setminus a$, *c.f.* line 4 of Algorithm 1. This yields S_i^+ , a positive subset of the lookup similarity matrix S .

As $|S^+| > m$ and one wants to extract the most distinctive descriptions from it, the selection heuristic Φ gets applied to S^+ . It selects top- m scoring descriptions via:

$$\text{top-}m(\text{mean}(S^+, \text{dim} = 0)), \quad (6)$$

i.e., those m descriptions whose averaged image-description similarity differences to c are, on average, maximally large. In other words, these are descriptions that activate high for a but not high for any $a' \in \mathcal{A} \setminus a$ on average. Because these m descriptions are selected without a prepended class name cls , they can serve as classname-free language representations of class c .

The selected descriptions can then be used as described in Section 3.2 or Section 3.1 for inference. In both cases, classification happens via an ensembling (classname-containing and classname-free) of image-language similarities, as introduced in (Radford et al. 2021). Applying arg max over the ensembled, description-enriched image-language similarities of the candidate set $\mathcal{A}(x_i)$ yields the final classification decision of the image.

Algorithm 1: Inference: Obtain distinctive language descriptions with feedback from VLM space.

Input: x_i - Query image to be evaluated

\mathcal{P} - global description pool obtained from previous stage

\mathcal{I} - probing image embeddings containing few n samples $\forall c \in \mathcal{C}$ in training split

\mathcal{A}_i - a set containing k preliminary labels using standard CLIP retrieval with only cls

Φ_m - selection heuristic to get m descriptions for \mathcal{A}_i from the pool

Output: set of distinctive language descriptions $\mathcal{D}_i \in \mathbb{N}^{k \times m}$

```

1:  $S \leftarrow \text{matmul}(\mathcal{I}, \mathcal{P}).\text{reshape}(n, |\mathcal{C}|, |\mathcal{P}|).\text{mean}(\text{dim} = 0) \in \mathbb{R}^{|\mathcal{C}| \times |\mathcal{P}|}$   $\triangleright$  Look-up similarity matrix
2:  $\mathcal{D}_i \leftarrow \{\}$ 
3: for each element  $a \in \mathcal{A}_i$  do
4:    $S_i^+ \leftarrow [S[a, :] - S[\mathcal{A}_i \setminus a, :]]^+$   $\triangleright$  Select the positive subset
5:    $\mathcal{D}_{i,a} \leftarrow \Phi_m(S_i^+) \in \mathbb{N}^m$   $\triangleright$  Extract  $m$  descriptions that distinguish  $a$  from the other  $\mathcal{A}_i$ 
6:    $\mathcal{D}_i \leftarrow \mathcal{D}_i \cup \mathcal{D}_{i,a}$   $\triangleright$  Descriptions to differentiate  $x_i$  from the  $k$  preliminary labels.
7:  $s(\mathcal{D}_i, x_i)$   $\triangleright$  Compute similarity within the local neighborhood

```

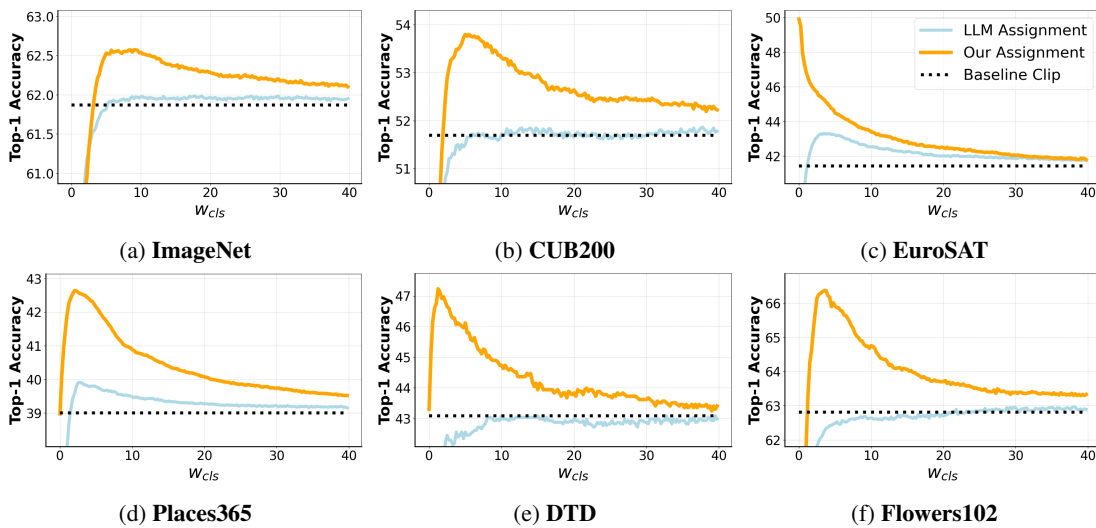


Figure 3: **Overall Performance of all datasets in classname-free setup.** For descriptions assigned by our method and an LLM, w_{cls} assesses the influence of class labels on the performance across different datasets. For a detailed discussion, see Section 4.2.

Better interpretability Our proposed method achieves *better interpretability* by offering these four characteristics:

1. **The original CLIP encoders for text and image are retained**, rather than fine-tuned to represent a different embedding space, as seen in some works (Zang et al. 2024; Feng, Bair, and Kolter 2023). Hence, our approach preserves the general validity of the CLIP embeddings.
2. **The number of resulting textual descriptions for a single class is kept within a reasonable limit**, similar to the approach in the seminal work (Menon and Vondrick 2022). This helps minimize the potential for noise augmentation, unlike methods that generate hundreds and thousands of descriptions (Esfandiarpoor and Bach 2024).
3. **The overlap between concepts across various classes is minimized**, in comparison to methods with global concept bottlenecks (Yang et al. 2023; Yan et al. 2023; Zang et al. 2024). Sparse overlapping ensures clearer distinc-

tions between classes.

4. **We do not use continuous weights over resulting textual descriptions**, as done in (Yang et al. 2023; Yan et al. 2023; Zang et al. 2024). Long vectors of continuous weights can be less interpretable compared to clear, discrete indicators of whether a concept is present. Hence, our method offers improved clarity and explainability.

4 Experiment

This section evaluates our approach on seven widely used benchmark datasets for (fine-grained) visual classification. We compare our approach to state-of-the-art methods and provide qualitative results.

4.1 Implementation Details and Datasets

Implementation details. We use CLIP (Radford et al. 2021) as the base Vision-Language Model (VLM) for our approach. Unless stated otherwise, the backbone for CLIP

Source of \mathcal{P}	Description Assignment	Max #desc. \downarrow	ImageNet	ImageNetV2	CUB200	EuroSAT	Places365	DTD	Flowers102
DCLIP	LLM assignments, global eval	13	61.99	55.09	51.79	43.31	39.91	43.09	62.97
DCLIP	LLM assignments, local top-k eval	13	61.99	55.06	51.83	43.29	39.87	43.09	62.86
DCLIP	<i>Ours</i>	5	<u>62.57</u>	55.48	53.80	49.89	<u>42.64</u>	47.23	<u>66.37</u>
Random Characters	<i>Ours</i>	5	62.18	<u>55.22</u>	52.31	40.82	40.44	44.73	66.12
Contrastive	LLM assignments	40	62.03	54.88	52.24	46.97	40.37	44.41	62.90
Contrastive	<i>Ours</i>	5	62.78	55.48	<u>53.45</u>	<u>49.47</u>	42.65	46.97	67.07

Table 1: **Image classification in classname-free setup.** Our method consistently produces the highest accuracies in this setting. To ensure a fair comparison, we use the best performing w_{cls} of the respective assignment.

is the ViT-B/32 (Vaswani et al. 2017; Dosovitskiy et al. 2020). We randomly sample a subset from each dataset’s standard training split to obtain the lookup similarity table S (details see Appendix A.10). Our empirical tests confirmed that this sampling process does not significantly impact performance. The Large-Language Model (LLM) generated descriptors are sourced directly from DCLIP (Menon and Vondrick 2022) or generated using the contrastive prompting method with gpt-3.5-turbo-1106 and Llama-3-70b-chat-hf via APIs.

Datasets. We evaluated our methods on the following standard datasets using the standard protocol (classification accuracy) based on previous works (Menon and Vondrick 2022; Roth et al. 2023): ImageNet (Deng et al. 2009), ImageNetV2 (Recht et al. 2019), CUB200-2011 (Wah et al. 2011) (fine-grained bird classification), EuroSAT (Helber et al. 2017) (satellite image recognition), Places365 (Zhou et al. 2017), DTD (Textures, (Cimpoi et al. 2014)), and Flowers102 (Nilsback and Zisserman 2008).

Source of obtaining description pool \mathcal{P} . These descriptions can be obtained in the following ways: 1) directly from the published descriptions of other works, such as DCLIP (Menon and Vondrick 2022) or FuDD (Esfandiarpoor and Bach 2024); 2) generated based on the provided procedures and code bases of other works, if descriptions are not available; 3) or created through contrastive prompting, which aims to extract meaningful descriptions by contrasting hard negative samples within a neighborhood. The motivation is similar to FuDD (Esfandiarpoor and Bach 2024), but we use significantly fewer descriptions per class. As this is only an alternative for constructing a description pool and orthogonal to our proposed method, we provide more details in Appendix A.8 on the construction of the contrastive pool.

4.2 Experimental Results

Classname-free evaluation. We evaluate the quality of the classname-free description assignments selected by our method in the classname-free evaluation setup (cf. Section 3.2). Examples of selected descriptions can be found in Appendix A.11. Performance of our algorithm across 7 classification benchmarks are shown in Figure 3, highlighting how varying w_{cls} impacts Top-1 accuracy. The non-ensembled CLIP baseline performance, independent of w_{cls} , is also included for reference. Our selected assignments consistently outperform the DCLIP LLM assignments. Notably, for the EuroSAT, Flowers102, CUB200, DTD, and

Places datasets, optimal performance occurs when w_{cls} is low ($[0, 10]$), emphasizing the importance of classname-free descriptions while exceeding the baseline performance by up to 9% and the LLM performance by up to 8%. However, the LLM-assigned descriptions cannot produce performance gains in the classname-free scenario that comes close to our selections.

Further increasing w_{cls} and thereby weighting the single classname-included description higher, reduces accuracy, showing that overly prioritizing the classname diminishes the benefits of our classname-free descriptions. Interestingly, the smaller gain for ImageNet (0.5pp.) also corresponds to a lower bump for low w_{cls} in the plot. This may be due to the noisier backgrounds of this dataset, which hinders selecting generally valid descriptions.

Quantitative results are shown in Table 1, where we report the peak accuracy for each dataset regardless of w_{cls} . Interestingly, only 5 selected classname-free descriptions per preliminary class of an image are enough to surpass the performance of the DCLIP LLM assignments. An additional classname-free performance of up to 6.6 pp. (for the EuroSAT dataset) can be achieved.

To confirm that our gains are not driven solely by the image-wise top- k neighborhood, we also evaluate DCLIP LLM assignments in the local top- k context, which shows no significant improvement. This suggests that our approach succeeds by the selection procedure within the top- k neighborhood rather than the search space restriction alone. Importantly, these gains are independent of a specific description pool \mathcal{P} as they hold for a contrastive prompting pool, too.

To our best knowledge, no prior work has explored a comparable classname-free evaluation setup to determine the true distinctiveness of assigned descriptions $d_0^{c-}, \dots, d_m^{c-}$ in combination with a classname prompt d^{c+} . However, some works use methods like trainable bottleneck classifiers (Yang et al. 2023; Yan et al. 2023) or trainable embeddings (Zang et al. 2024), which can be considered "classname-free." Despite this similarity, they are too different to compare against (detailed discussion in Appendix A.9).

Conventional setup. We evaluate our chosen descriptions in a conventional setup where classnames are included in all descriptions, as shown in Table 3. Our method performs well on datasets where a higher bump in performance is observed with low w_{cls} , i.e. high relative description weights

Description assignment	ImageNet	ImageNetV2	CUB200	EuroSAT	Places365	DTD	Flowers102
LLM assignments	11.65	10.69	3.47	28.11	21.36	17.77	3.19
random assignments	0.08	0.06	0.43	11.61	0.11	2.45	1.01
<i>Ours</i>	50.16	43.98	41.53	43.24	36.36	43.09	51.52

Table 2: **Performance in classname-free setup with $w_{cls} = 0$.** Our descriptions are robust enough and perform decently, even if the classname text D_{cls} is weighted by $w_{cls} = 0$. LLM assignments give a considerably worse performance in this scenario. Randomly assigned descriptions fail to provide reasonable guidance. Llama3-70B with Contrastive prompt is used as source pool \mathcal{P} .

Method	Source of \mathcal{P}	Max #desc. \downarrow	ImageNet	ImageNetV2	CUB200	EuroSAT	Places365	DTD	Flowers102
CLIP	-	1	61.87	54.74	51.69	40.92	39.01	43.09	62.81
DCLIP	DCLIP	12	62.22	54.84	52.55	47.33	40.01	41.86	62.17
WaffleClip	WaffleClip	30	63.31	55.92	52.38	44.31	40.56	43.16	66.27
FuDD	FuDD	1842	64.19	56.75	54.30	45.18	42.17	44.84	67.62
<i>Ours</i>	DCLIP	5	61.59	53.61	55.89	50.05	42.77	48.83	66.99
<i>Ours</i>	Contrastive	20	63.30	55.24	56.27	58.57	43.65	48.09	68.61
<i>Ours</i>	FUDD	25	61.86	53.05	56.62	48.42	42.76	48.03	68.47
<i>Ours</i>	Contrastive	50	63.51	55.41	56.45	44.46	43.62	47.66	69.51

Table 3: **Image classification with classname included in the descriptions.** An ablation of ambiguous context size k can be found in Appendix A.6.

LLMs	ImageNet	ImageNetV2	CUB200	EuroSAT	Places365	DTD	Flowers102
Contrastive Llama3-70B	61.68	54.64	53.49	36.33	41.33	79.87	64.45
w/ Our Selection	63.30	55.24	56.27	58.57	43.65	48.09	68.61

LLMs	ImageNet	ImageNetV2	CUB200	EuroSAT	Places365	DTD	Flowers102
Contrastive GPT3.5	61.65	54.69	53.83	35.38	40.79	44.10	66.29
w/ Our Selection	63.15	55.09	56.21	44.43	43.64	80.78	68.48

Table 4: **Performance of classname-included descriptions: LLM assignments vs Our selection assignments.**

in Figure 3. This happens when the selected description pool provides generalizable, diverse, and discriminative descriptions for the datasets. Our method outperforms DCLIP assignments in the DCLIP pool and outdoes WaffleClip and FuDD on datasets CUB200, EuroSAT, Places365, DTD, and Flowers102. This remains true for 4 of these datasets, even if only 5 descriptions per class are used. In contrast, WaffleClip (Roth et al. 2023) uses 30 text prompts per class, and FuDD (Esfandiarpoor and Bach 2024) uses an astonishing number of 1,842 descriptions per class.

On the other hand, for ImageNet and ImageNetV2, we can see a connection between suboptimal conventional performance and a much lower peak relative to baseline CLIP in the classname-free setting - indicating less distinctive power of our assignments. Mixed results in the conventional setup for ImageNet and ImageNetV2 imply it is challenging to find distinctive descriptions - at least within the currently used description pools \mathcal{P} . This difficulty may arise because random image contents, e.g. background objects, distort the description assignments. Our algorithm experiences a performance boost when using a \mathcal{P} obtained through contrastive prompting, offering a richer pool of descriptions.

Overall, the results from the class name-containing scenario suggest that the added semantics of the discovered descriptions enhance performance—in addition to the class name ensembling used by other methods like WaffleClip, FuDD, and DCLIP.

Performance in classname-free scenario when $w_{cls} = 0$. We evaluate the performance under a classname-free scenario in Table 2 without using any guiding classname information. In this case, random assignments don't achieve any reasonable classification accuracy; LLM-assigned descriptions provide minor guidance. With our selected descriptions, however, we have achieved decent performance across all datasets - significantly surpassing the LLM assignments. This further supports the idea that descriptions assigned by an LLM are not distinctive enough. Instead, feedback from the embedding space is needed for distinctive assignments.

Combined with different LLMs. Table 4 demonstrates that our algorithm functions effectively with contrastively obtained description pools from both LLMs LlaMa and ChatGPT. This illustrates the versatility of our method.

5 Conclusion

In our study, we found that *VLM Classification performance does indeed benefit from LLM description semantics - if the descriptions are correctly selected*. For that, we present a new, training-free approach that assigns semantically meaningful descriptions based on feedback from the VLM embedding space. We show that descriptions assigned in this way do have discriminative power on their own, *i.e.* when evaluated in our proposed setup that has no classname ensembling. These description assignments improve the performance in image classification tasks - with and without classname ensembling. Furthermore, this evaluation setup helps to differentiate performance gains from genuine semantics versus gains from ensemble effects. Hopefully, our findings inspire future work on VLMs and model interpretability.

References

Belinkov, Y.; and Bisk, Y. 2018. Synthetic and Natural Noise Both Break Neural Machine Translation. In *ICLR*.

Brown, T.; Mann, B.; Ryder, N.; Subbiah, M.; Kaplan, J. D.; Dhariwal, P.; Neelakantan, A.; Shyam, P.; Sastry, G.; Askell, A.; et al. 2020. Language models are few-shot learners. *Advances in neural information processing systems*, 33: 1877–1901.

Chen, J.; Yang, Z.; and Yang, D. 2020. MixText: Linguistically-Informed Interpolation of Hidden Space for Semi-Supervised Text Classification. In *ACL*.

Cimpoi, M.; Maji, S.; Kokkinos, I.; Mohamed, S.; and Vedaldi, A. 2014. Describing Textures in the Wild. In *CVPR*.

Cohen, J. M.; Rosenfeld, E.; and Kolter, J. Z. 2019. Certified adversarial robustness via randomized smoothing. *arXiv preprint arXiv:1902.02918*.

Deng, J.; Dong, W.; Socher, R.; Li, L.-J.; Li, K.; and Fei-Fei, L. 2009. Imagenet: A large-scale hierarchical image database. In *CVPR*.

Dosovitskiy, A.; Beyer, L.; Kolesnikov, A.; Weissenborn, D.; Zhai, X.; Unterthiner, T.; Dehghani, M.; Minderer, M.; Heigold, G.; Gelly, S.; et al. 2020. An image is worth 16x16 words: Transformers for image recognition at scale. *arXiv preprint arXiv:2010.11929*.

Esfandiarpoor, R.; and Bach, S. H. 2024. Follow-Up Differential Descriptions: Language Models Resolve Ambiguities for Image Classification. *ICLR*.

Feng, S. Y.; Gangal, V.; Wei, J.; Chandar, S.; Vosoughi, S.; Mitamura, T.; and Hovy, E. 2021. A survey of data augmentation approaches for NLP. *arXiv preprint arXiv:2105.03075*.

Feng, Z.; Bair, A.; and Kolter, J. Z. 2023. Text Descriptions are Compressive and Invariant Representations for Visual Learning. *arXiv:2307.04317*.

Hakimov, S.; and Schlangen, D. 2023. Images in Language Space: Exploring the Suitability of Large Language Models for Vision & Language Tasks. In Rogers, A.; Boyd-Graber, J.; and Okazaki, N., eds., *Findings of the Association for Computational Linguistics: ACL 2023*. Toronto, Canada: Association for Computational Linguistics.

Hao, X.; Zhu, Y.; Appalaraju, S.; Zhang, A.; Zhang, W.; Li, B.; and Li, M. 2023. Mixgen: A new multi-modal data augmentation. In *WACV*.

Helber, P.; Bischke, B.; Dengel, A.; and Borth, D. 2017. EuroSAT: A Novel Dataset and Deep Learning Benchmark for Land Use and Land Cover Classification. *IEEE Journal of Selected Topics in Applied Earth Observations and Remote Sensing*.

Jin, H.; Li, Z.; Tong, R.; and Lin, L. 2018. A deep 3D residual CNN for false-positive reduction in pulmonary nodule detection. *Medical physics*, 45(5): 2097–2107.

Kobayashi, S. 2018. Contextual Augmentation: Data Augmentation by Words with Paradigmatic Relations. In *NAACL-HLT*.

Li, J.; Selvaraju, R.; Gotmare, A.; Joty, S.; Xiong, C.; and Hoi, S. C. H. 2021. Align before fuse: Vision and language representation learning with momentum distillation. *Advances in neural information processing systems*, 34: 9694–9705.

Li, L. H.; Yatskar, M.; Yin, D.; Hsieh, C.-J.; and Chang, K.-W. 2019. Visualbert: A simple and performant baseline for vision and language. *arXiv preprint arXiv:1908.03557*.

Lin, T.-Y.; Maire, M.; Belongie, S.; Hays, J.; Perona, P.; Ramanan, D.; Dollár, P.; and Zitnick, C. L. 2014. Microsoft coco: Common objects in context. In *Computer Vision–ECCV 2014: 13th European Conference, Zurich, Switzerland, September 6–12, 2014, Proceedings, Part V 13*, 740–755. Springer.

Menon, S.; and Vondrick, C. 2022. Visual Classification via Description from Large Language Models. *arXiv:2210.07183*.

Nilsback, M.-E.; and Zisserman, A. 2008. Automated Flower Classification over a Large Number of Classes. In *Indian Conference on Computer Vision, Graphics and Image Processing*.

Ouyang, L.; Wu, J.; Jiang, X.; Almeida, D.; Wainwright, C.; Mishkin, P.; Zhang, C.; Agarwal, S.; Slama, K.; Ray, A.; et al. 2022. Training language models to follow instructions with human feedback. *Advances in neural information processing systems*, 35: 27730–27744.

Pratt, S.; Covert, I.; Liu, R.; and Farhadi, A. 2023. What does a platypus look like? Generating customized prompts for zero-shot image classification. *arXiv:2209.03320*.

Radford, A.; Kim, J. W.; Hallacy, C.; Ramesh, A.; Goh, G.; Agarwal, S.; Sastry, G.; Askell, A.; Mishkin, P.; Clark, J.; et al. 2021. Learning transferable visual models from natural language supervision. In *ICML*.

Recht, B.; Roelofs, R.; Schmidt, L.; and Shankar, V. 2019. Do imagenet classifiers generalize to imagenet? In *International conference on machine learning*, 5389–5400. PMLR.

Roth, K.; Kim, J. M.; Koepke, A.; Vinyals, O.; Schmid, C.; and Akata, Z. 2023. Waffling around for performance: Visual classification with random words and broad concepts. In *Proceedings of the IEEE/CVF International Conference on Computer Vision*, 15746–15757.

Şahin, G. G. 2022. To Augment or Not to Augment? A Comparative Study on Text Augmentation Techniques for Low-Resource NLP. *Computational Linguistics*.

Sun, L.; Xia, C.; Yin, W.; Liang, T.; Philip, S. Y.; and He, L. 2020. Mixup-Transformer: Dynamic Data Augmentation for NLP Tasks. In *Computational Linguistics*.

Szegedy, C.; Liu, W.; Jia, Y.; Sermanet, P.; Reed, S.; Anguelov, D.; Erhan, D.; Vanhoucke, V.; and Rabinovich, A. 2015. Going deeper with convolutions. In *Proceedings of the IEEE conference on computer vision and pattern recognition*, 1–9.

Touvron, H.; Martin, L.; Stone, K.; Albert, P.; Almahairi, A.; Babaei, Y.; Bashlykov, N.; Batra, S.; Bhargava, P.; Bhosale, S.; et al. 2023. Llama 2: Open foundation and fine-tuned chat models. *arXiv preprint arXiv:2307.09288*.

Vaswani, A.; Shazeer, N.; Parmar, N.; Uszkoreit, J.; Jones, L.; Gomez, A. N.; Kaiser, Ł.; and Polosukhin, I. 2017. Attention is all you need. *Advances in neural information processing systems*, 30.

Vogel, F.; Shvetsova, N.; Karlinsky, L.; and Kuehne, H. 2022. VL-Taboo: An Analysis of Attribute-based Zero-shot Capabilities of Vision-Language Models. arXiv:2209.06103.

Wah, C.; Branson, S.; Welinder, P.; Perona, P.; and Belongie, S. 2011. The Caltech-UCSD Birds-200-2011 Dataset. Technical report, California Institute of Technology.

Yan, A.; Wang, Y.; Zhong, Y.; Dong, C.; He, Z.; Lu, Y.; Wang, W.; Shang, J.; and McAuley, J. 2023. Learning Concise and Descriptive Attributes for Visual Recognition. arXiv:2308.03685.

Yang, Y.; Panagopoulou, A.; Zhou, S.; Jin, D.; Callison-Burch, C.; and Yatskar, M. 2023. Language in a Bottle: Language Model Guided Concept Bottlenecks for Interpretable Image Classification. arXiv:2211.11158.

Young, P.; Lai, A.; Hodosh, M.; and Hockenmaier, J. 2014. From image descriptions to visual denotations: New similarity metrics for semantic inference over event descriptions. *Transactions of the Association for Computational Linguistics*, 2: 67–78.

Zang, Y.; Yun, T.; Tan, H.; Bui, T.; and Sun, C. 2024. Pre-trained Vision-Language Models Learn Discoverable Visual Concepts. arXiv:2404.12652.

Zhang, J.; Huang, J.; Jin, S.; and Lu, S. 2024. Vision-language models for vision tasks: A survey. *IEEE Transactions on Pattern Analysis and Machine Intelligence*.

Zhao, T.; Zhang, T.; Zhu, M.; Shen, H.; Lee, K.; Lu, X.; and Yin, J. 2022. An Explainable Toolbox for Evaluating Pre-trained Vision-Language Models. In Che, W.; and Shutova, E., eds., *Proceedings of the 2022 Conference on Empirical Methods in Natural Language Processing: System Demonstrations*, 30–37. Abu Dhabi, UAE: Association for Computational Linguistics.

Zhou, B.; Lapedriza, A.; Khosla, A.; Oliva, A.; and Torralba, A. 2017. Places: A 10 million Image Database for Scene Recognition. *T-PAMI*.

Zhou, K.; Yang, J.; Loy, C. C.; and Liu, Z. 2022. Learning to Prompt for Vision-Language Models. *International Journal of Computer Vision*, 130(9): 2337–2348.

A Appendix

A.1 Limitations and Ethical Considerations

Currently, most of the methods in this domain, including ours, work with a fixed pool of descriptions \mathcal{P} from LLMs. Although our method finds precise and meaningful descriptions for better performance, it would be interesting to give such selection feedback to LLMs and let them refine the \mathcal{P} in an agentic fashion. Furthermore, due to resource limitations, we could not test our method on a more diverse and scalable dataset. However, we anticipate it will still perform well. We are not aware of any ethical considerations, currently.

A.2 Different choices of size k and n

Table 5 ablates the number k of preliminary labels per test image and n , the number of images per class available in the selection set for S . Results were obtained in the classname-included evaluation setup on the CUB200 Dataset with 5 selected descriptions from the DClip description pool. Increasing the number of selection samples in S leads to increasing performances. For the CUB dataset, the optimal k value is empirically found to be $k = 3$ as it has a right trade-off between a diverse set of candidates that is still small enough to find distinctive descriptions inside. This shows that even in a few-shot regime with only 5 selected descriptions per candidate class baselines such as (Esfandiarpoor and Bach 2024) and (Menon and Vondrick 2022) can be exceeded (cf. Table 3 in the main text).

n / k	2	3	4
5	53.33	54.00	54.04
10	54.38	55.20	54.31
15	54.85	55.63	55.51
20	55.28	55.82	55.75
25	55.70	55.59	55.44

Table 5: **Hyper-params comparison on CUB200 dataset for ViT-B/32 backbone** k defines the number of preliminary labels per test image to consider, and n denotes the number of images per class available in the selection set for S .

A.3 Choice of heuristics.

Table 6 shows the results when different $\Phi(\cdot, \cdot)$ is applied. On datasets that work well under classname-free scenario (see Figure 3), *i.e.* shows the characteristic bump for w_{cls} in $[0, 10]$, the maxmean heuristic works better. On datasets where this bump is absent (ImageNet, Food101, and Oxford Pets), the maxmin heuristic performs better. This can come from the fact that finding descriptions that distinguish one preliminary class from all others simultaneously is challenging for these datasets. Since the maxmin heuristic focuses on maximizing the smallest similarity difference, future works should explore pairwise comparisons to mine descriptions for these datasets.

Heuristics $\Phi(\cdot, \cdot)$	ImageNetV2	ImageNet	CUB200	EuroSAT	Places365
maxmean	60.13	60.09	55.16	49.30	41.60
maxmin	61.05	60.60	51.95	49.58	40.26

Table 6: **Choice of the selection heuristics $\Phi(\cdot, \cdot)$**

A.4 Ablation for description assignments with \mathcal{P} from DCLIP.

An intriguing experiment investigates what happens if descriptions get assigned randomly to classes. Table 7 compares LLM assignments to random assignments and the assignments of our method in the classname-free setup. The assignments are evaluated both on a global scale, without restricting the classification to local candidates, and a local top- k candidate neighborhood (cf. Algorithm 1). As can be seen, the LLM assignments provide some guidance but not reliably so. They perform similarly to random assignments, and even for 2 datasets random descriptions can surpass the LLM assignments. The effect of the local candidate evaluation for random and LLM assignments is restricted (rows 2 and 4), as their description assignments are not adjusted to the local candidate set. On the other hand, our assignments constantly offer the best results.

Description assignment	Max #desc.	ImageNet	ImageNetV2	CUB200	EuroSAT	Places365	DTD	Flowers102
LLM assignments, global eval	13	61.09	55.00	51.79	43.31	39.91	43.09	62.97
LLM assignments, local top-k eval	13	61.09	55.06	51.83	43.29	39.87	43.09	62.86
random assignments, global eval	13	61.88	54.86	52.00	41.46	38.98	43.24	62.81
random assignments, local top-k eval	13	61.91	54.86	51.97	41.41	39.02	43.30	62.82
<i>Ours</i>	5	62.57	55.48	53.80	49.89	42.64	47.23	66.37

Table 7: **Ablation for assignment with \mathcal{P} from DCLIP.** Evaluation under the classname-free setup.

A.5 Results for ViT-L/14 CLIP Backbone

We also show evaluation results on the ViT-L/14 CLIP backbone, as it is commonly used for an additional comparison. One can see a consistent pattern as we showed in the main paper for the ViT-B/32. Cf. Table 9 and Table 8.

A.6 Ablating ambiguous context size k

Table 10 ablates parameter k , which denotes the number of ambiguous classes considered per test image x_i . Different datasets behave differently under a changed k . Interestingly, datasets with challenging description behavior - namely Food101, ImageNet and ImageNetV2- do not show a high sensitivity to a varying k . The best and worst performances for these datasets do not differ much, although a tendency for slightly better performances for higher values of k can be observed. The remaining datasets with favorable description behavior are much more sensitive to the chosen values of k : CUB200 and EuroSAT¹ perform best for low values of k while DTD, Flowers102 and Places365 perform best for medium to high values of k . However, for any chosen value of k , LLM assignments are surpassed significantly for these datasets. Similar results are confirmed in Table 11 for the ViT-L/14 backbone where Food101, ImageNet, and

¹In this evaluation $n = 2000$ *vs.* $n = 1000$ in Table 3. The reduced bias explains the stronger results.

Method	Source of \mathcal{P}	Max #des	ImageNet	ImageNetV2	CUB200	EuroSAT	Places365	Food101	Oxford Pets	DTD	Flowers102
CLIP	-	1	73.43	67.86	62.22	55.02	40.62	90.75	93.24	52.45	74.81
DCLIP	DCLIP	12	74.47	68.74	63.39	57.97	41.66	89.94	93.51	54.73	76.83
WaffleClip	WaffleClip	30	75.30	69.48	64.18	61.17	42.26	93.31	91.98	53.94	-
FuD (k = C)	FuD	1842	77.00	71.05	66.03	60.64	44.09	94.27	93.51	57.23	79.67
<i>Ours</i>	DCLIP	5	74.37	68.15	67.79	65.05	44.16	90.11	93.05	58.83	79.69
<i>Ours</i>	DCLIP	50	75.62	69.70	68.55	63.71	45.00	91.54	93.59	59.57	81.05
<i>Ours</i>	Contr. Pr.	50	76.04	69.79	69.07	62.77	45.20	91.34	93.43	59.57	80.96

Table 8: **Image classification with classname-included descriptions for ViT-L-14 backbone.**

Source of \mathcal{P}	Description Assignment	Max #desc. \downarrow	ImageNet	ImageNetV2	CUB200	EuroSAT	Places365	Food101	Oxford Pets	DTD	Flowers102
DCLIP	LLM assignments	12	73.66	68.05	63.07	56.85	41.54	90.80	93.32	53.56	74.84
DCLIP	<i>Ours</i>	5	74.55	68.91	65.59	56.08	44.21	90.92	93.35	57.23	80.45
Contrastive	LLM assignments	40	73.57	68.04	62.82	55.91	41.85	90.82	93.73	54.84	75.09
Contrastive	random assignments	40	73.07	67.96	63.38	56.39	40.62	90.78	93.24	52.87	74.86
Contrastive	<i>Ours</i>	5	74.61	68.70	66.59	55.68	44.34	91.02	93.30	56.97	80.45

Table 9: **Image classification in classname-free setup for ViT-L-14 backbone.** Maximum value for the best performing w_{cls} per cell.

ImageNetV2 classification performance reacts insensitively to k . Interestingly, for ViT-L/14, high k values benefit the classification performance, whereas for ViT-B/32, low k values yielded the best results.

Besides that, it is remarkable that the language-maxing accuracy denoted in parentheses closely matches or even surpasses² the ensembling accuracy, although it cannot make use of the smoothing ensembling effect that can work with random descriptions (see Appendix A.7). This points to the distinctive quality of the selected descriptions.

A.7 Evaluating Beyond Ensembling

Knowing that ensemble effects can boost classification accuracy with non-semantic descriptions, such as random strings, that serve to obtain alternative classname embeddings, an interesting ablation involves eliminating the ensembling from the evaluation process. The ensembling evaluation of image x worked via $\tilde{c} = \arg \max_{c \in \mathcal{C}} s(c, x)$ with $s(c, x) = \frac{1}{|\mathcal{D}(c)|} \sum_{d \in \mathcal{D}(c)} \phi(e(d), e(x))$. The ensembling can be eliminated by using $\tilde{c} = \arg \max_{c \in \mathcal{C}} s(c, x)$ as before but with $s(c, x) = \max_{d \in \mathcal{D}(c)} \phi(e(d), e(x))$ which denotes the maximum image-description similarity of candidate class c . This way, no smoothing averaging operation is involved. A maximum operator replaces it. Hence, it can be conjectured that this evaluation procedure is semantics-sensitive, provided that the vision-language embedding space correctly embeds textual description semantics.

Table 12 compares the results of both evaluation modes within the DCLIP description pool. It shows that within the DCLIP description pool, the baseline - Ensembling of classwise DCLIP LLM assignments - is *only* exceeded by the selected assignments of the proposed method. The gains are considerable, reaching from **+3.15** to up to **+9.81**. These results are achieved, although the maxing evaluation is ensembling-free. Hence, no use can be made of ensembling effects that boost performances independently of description semantics. On the other hand,

²In case of the ViT-L/14 backbone.

when applying the maxing evaluation protocol to the LLM-assigned descriptions, the classification accuracy drops for 6/7 datasets investigated. Focusing on the highest activating ``{cls}, {description}''-embedding hampers the classification accuracy when the assignments $\text{cls} \leftrightarrow \text{description}$ are obtained by an LLM. In contrast, if these assignments are obtained from the proposed selection method, a considerable performance boost to the ensembling baseline can be observed for 5/7 datasets. For both datasets, ImageNet and ImageNetV2, no performance boost can be observed when maxing. This also holds for the LLM-assigned descriptions and points to the fact that ImageNet and ImageNetV2 show less sensitivity to description semantics, as already pointed out in Table 1.

A.8 Construction of the description pool \mathcal{P} from existing method.

To construct the description pool \mathcal{P} , one source is to utilize published descriptions from other works, such as DCLIP (Menon and Vondrick 2022). However, since DCLIP does not provide descriptions for Flowers102, we generated descriptions for this dataset using GPT-3.5 with prompts from their code base. In these scenarios, the LLM "assigns" descriptions to a class by generating them specifically for that class. Therefore, both LLM assignments and our assignments, as described in Algorithm 1, are included in the DCLIP description pool. In rare instances where the LLM did not return a description following the DCLIP approach, a neutral description, such as "a kind of food" for the food dataset, was used. This step was necessary to avoid distorting the results in this setup otherwise.

Contrastive prompting As the vanilla CLIP model can locate the image embedding in an approximate correct neighborhood already with only `cls` provided, we can use this information to find out the classes that are usually misclassified to each other. Instead of defining ambiguous classes for each image, we obtain the contrastive description pool with a statistical sample of ambiguous classes for each

ViT-B/32		Test Dataset								
k		CUB200	DTD	EuroSAT	Flowers102	Food101	ImageNet	ImageNetV2	Oxford Pets	Places365
2		55.90 (55.01)	46.17 (45.64)	55.39 (55.57)	66.11 (66.97)	80.34 (80.59)	61.64 (62.38)	54.10 (54.95)	83.57 (84.11)	42.27 (42.05)
3		55.89 (55.63)	48.83 (48.09)	53.41 (53.10)	66.99 (68.29)	80.09 (80.27)	61.58 (62.00)	53.61 (54.42)	82.77 (84.16)	42.77 (42.49)
4		55.13 (55.44)	49.57 (48.78)	48.63 (51.30)	67.54 (67.80)	80.06 (80.28)	61.32 (61.76)	53.51 (53.85)	82.86 (83.76)	42.90 (42.42)
5		55.78 (55.40)	50.05 (49.26)	49.00 (51.81)	67.49 (68.12)	80.11 (80.25)	61.10 (61.58)	53.43 (54.06)	82.15 (83.32)	42.83 (42.27)
6		55.64 (54.92)	50.05 (48.14)	48.19 (53.36)	68.06 (68.27)	79.91 (80.10)	61.25 (61.39)	53.63 (54.04)	81.96 (82.99)	42.82 (42.33)
7		55.28 (55.07)	49.89 (47.77)	49.14 (53.23)	68.79 (68.71)	80.06 (80.17)	61.30 (61.46)	53.61 (54.02)	82.31 (82.34)	42.75 (42.24)
8		55.28 (54.64)	50.74 (47.77)	51.06 (52.16)	68.74 (68.30)	79.99 (80.24)	61.34 (61.44)	53.91 (54.02)	82.31 (82.67)	42.69 (42.06)
9		54.80 (54.61)	50.80 (47.55)	51.57 (49.33)	68.84 (68.40)	80.07 (80.31)	61.25 (61.44)	53.79 (53.81)	82.31 (82.45)	42.84 (42.21)
10		54.61 (54.49)	50.37 (47.18)	51.94 (50.26)	69.13 (68.66)	80.23 (80.28)	61.39 (61.37)	53.74 (53.80)	82.69 (82.69)	42.75 (42.09)
15		54.50 (53.56)	50.05 (47.18)	-	69.87 (68.73)	80.49 (80.24)	61.59 (61.50)	53.95 (53.78)	83.59 (83.78)	42.82 (42.08)
20		53.85 (52.88)	49.68 (46.54)	-	70.14 (68.47)	80.55 (79.92)	61.56 (61.26)	53.84 (53.61)	84.60 (84.85)	43.07 (42.13)
25		53.54 (52.59)	49.68 (47.29)	-	70.14 (69.07)	80.52 (79.55)	61.60 (61.14)	54.16 (53.51)	84.00 (84.44)	42.87 (41.88)
30		53.30 (52.49)	49.20 (46.49)	-	69.90 (69.30)	80.37 (79.47)	61.71 (61.17)	54.19 (53.47)	84.03 (84.30)	42.85 (41.77)
LLM Assignments		52.55	41.86	47.33	62.17	79.64	62.22	54.84	84.66	40.01
Maximum Gain in pp.		3.45	8.94	8.24	7.97	0.95	0.16	0.11	0.19	3.06

Table 10: **Evaluation of k in the classname containing setup for ViT-B/32.** Ensembling accuracy and language-maxing accuracy in parentheses. Datasets with challenging description behavior - namely Food101, ImageNet, ImageNetV2 and OxfordPets - tend to perform best for high values of k . The remaining datasets with favorable description behavior show no uniform pattern but significantly surpass the LLM-assigned baseline. LLM-assigned performance for reference. An evaluation is impossible where $k > |\mathcal{C}|$ (denoted by -). Used parameters: pool = DCLIP, $m = 5$, $n = \text{maximal}$.

ViT-L/14		Test Dataset								
k		CUB200	DTD	EuroSAT	Flowers102	Food101	ImageNet	ImageNetV2	Oxford Pets	Places365
2		67.28 (67.29)	58.51 (57.71)	59.20 (57.81)	78.83 (77.93)	90.07 (90.30)	74.16 (74.38)	68.27 (68.72)	91.88 (92.53)	43.68 (43.58)
3		67.81 (67.09)	58.83 (57.87)	60.56 (56.56)	79.69 (79.53)	90.11 (89.85)	74.36 (74.28)	68.15 (68.32)	93.05 (92.61)	44.16 (44.03)
4		67.02 (66.86)	59.26 (58.56)	62.26 (58.04)	80.40 (80.14)	90.19 (89.66)	74.32 (74.29)	68.55 (68.20)	92.83 (92.20)	44.48 (44.08)
5		66.83 (66.93)	60.27 (58.88)	62.81 (58.61)	80.87 (80.39)	90.10 (89.68)	74.55 (74.22)	68.40 (68.18)	92.12 (91.93)	44.46 (43.99)
6		66.52 (66.10)	59.79 (58.99)	63.46 (59.69)	81.40 (80.52)	90.19 (89.57)	74.49 (74.04)	68.79 (68.36)	91.85 (91.50)	44.45 (43.79)
7		67.40 (66.09)	60.16 (59.20)	63.46 (60.86)	82.01 (80.94)	90.26 (89.62)	74.54 (74.06)	68.30 (68.33)	91.50 (91.14)	44.48 (43.80)
8		66.97 (66.19)	60.05 (59.20)	64.73 (64.83)	82.29 (81.28)	90.22 (89.77)	74.49 (73.95)	68.33 (68.35)	91.17 (90.76)	44.44 (43.58)
9		66.62 (65.57)	61.12 (58.99)	65.57 (66.26)	82.66 (81.53)	90.17 (89.81)	74.57 (73.97)	68.62 (68.00)	90.62 (90.24)	44.52 (43.67)
10		66.33 (65.57)	61.01 (58.94)	66.53 (65.51)	82.76 (82.13)	90.21 (89.68)	74.57 (73.97)	68.40 (68.01)	90.65 (89.75)	44.62 (43.59)
15		66.17 (64.83)	61.70 (60.05)	-	82.48 (82.05)	90.37 (89.64)	74.58 (73.93)	68.56 (67.73)	90.62 (89.75)	44.65 (43.41)
20		65.34 (63.69)	61.22 (58.62)	-	81.05 (80.53)	90.28 (89.37)	74.56 (73.76)	68.42 (67.64)	90.71 (89.94)	44.47 (43.32)
25		65.43 (63.41)	61.17 (58.56)	-	81.10 (80.39)	90.04 (89.19)	74.63 (73.75)	68.63 (67.69)	91.36 (90.46)	44.32 (42.98)
30		65.14 (63.24)	61.01 (57.66)	-	81.07 (80.61)	89.85 (88.99)	74.56 (73.53)	68.61 (67.49)	90.92 (90.13)	44.17 (42.81)
LLM Assignments		63.39	54.73	57.97	76.83	89.94	74.47	68.74	93.51	41.66
Maximum Gain in pp.		4.42	6.97	8.56	5.93	0.43	0.09	-0.02	-0.46	2.99

Table 11: **Evaluation of k in the classname containing setup for ViT-L/14.** Ensembling accuracy and language-maxing accuracy in parentheses. Datasets with challenging description behavior - namely Food101, ImageNet, ImageNetV2 and OxfordPets - tend to perform best for high values of k while performing on par with the LLM-assigned baseline. The remaining datasets with favorable description behavior show no uniform pattern but significantly surpass the LLM-assigned baseline. An evaluation is impossible where $k > |\mathcal{C}|$ (denoted by -). Used parameters: pool = DCLIP, $m = 5$, $n = \text{maximal}$.

Classification Accuracies for ViT-B/32									
Description Pool	Assignment	Evaluation Mode	ImageNet	ImageNetV2	CUB200	EuroSAT	Places365	DTD	Flowers102
DCLIP	LLM	Ensembling	55.82	63.12	52.47	43.29	40.47	43.99	64.01
DCLIP	LLM	Maxing	54.41 (-1.41)	61.67 (-1.45)	52.40 (-0.07)	43.29 (0)	37.21 (-3.26)	43.35 (-0.63)	63.62 (-0.39)
DCLIP	Selected	Maxing	54.42 (-1.40)	62.00 (-1.12)	55.62 (3.15)	53.10 (9.81)	42.49 (2.02)	48.08 (4.09)	68.28 (4.27)

Table 12: **Comparison of semantic-sensitive maxing evaluation for both assignment types within the DCLIP description pool.** Evaluation happens in the classname-containing, conventional scenario to compare the classname ensembling effect to the non-ensembling maxing evaluation. Ensembling of LLM-assigned descriptions is referenced as a baseline. Colored differences between maxing evaluation and baseline performance are displayed. For LLM-assigned descriptions, maxing performance falls short of the ensembling baseline performance in 6/7 cases and exceeds it in no case. Contrary to this, the maxing evaluation for the selected assignments exceeds ensembling baseline performance in 5/7 cases with considerable gains. Thus, the enhanced semantic distinctiveness of the selected descriptions enables to surpass the classname ensembling effect.

class $c \in \mathcal{C}$. All the pairs $\forall c \in \mathcal{C} : \forall a \in \mathcal{A}(c) : (c, a)$, where we know which classes are usually miss-classified by CLIP solely based on `cls`. This information is then used to prompt an LLM to generate distinguishing attributes between c and a . For each class in its both possible roles c and a , all the generated descriptions obtained in this way get collected. This yields an LLM-assignment $\forall c \in \mathcal{C} : \mathcal{D}(c)_{LLM}$. The LLM assignments can be removed to obtain a global description pool \mathcal{P} without any assignments $\mathcal{D}(c)$. The global pool then allows the application of Algorithm 1, which yields class assignments $\mathcal{D}(c)$ per image x_i based on feedback from the VLM embedding space.

A.9 Comparison to prior works in the classname-free setting

As briefly discussed in the main text, we are the first to search and evaluate distinctive classname-free textual descriptions in a VLM ensembling scenario. However, some studies have employed trainable bottlenecks or distorted the underlying embedding space in classname-free scenarios. The differences are discussed below:

- Works like *LaBo* (Yang et al. 2023) use large Bottleneck sizes (from 500 for CUB up to 50,000 for ImageNet). They are mostly larger than the original CLIP embedding dimensionality, cf. Table 16 in the appendix of (Yang et al. 2023)). Therefore, the CLIP image embedding gets transformed to an overcomplete basis and overlaps 100% between classes. This requires that several thousands of continuous linear classifier weights be interpreted for every class, which is quite cumbersome.
- In the case of *Concise and descriptive Descriptions* (Yan et al. 2023), the Bottleneck size is much smaller than in LaBo, e.g. 64. However, the Bottleneck is still shared totally among all the classes, and one has to interpret a vector of 64 continuous weights per class.
- In the case of *Pre-trained vision-language models learn discoverable visual concepts* (Zang et al. 2024), the bottleneck sizes are quite large, though the associated weights are more interpretable as they are only elements of 0, 1. However, the text and image embeddings both get projected through a linear layer first, thus leaving the original, generally valid CLIP space. This raises questions about the general validity of the used image-language similarities.

(Vogel et al. 2022) evaluated VLM classification by relying only on language descriptions but did not analyze the interplay between *separate* descriptions and a simultaneously introduced classname prompt d^{c+} , which is crucial to understand the resulting accuracy in VLM ensembling scenarios. In addition to that, every image description was appended to the same text prompt. The resulting long prompts degraded performance.

A.10 Chosen selection sizes n

Dataset	n
CUB 200	29
DTD	40
Eurosat	1000
Flowers 102	20
ImageNet	732
ImageNetV2	732

Table 13: **Number of Image Samples per class n used to construct the selection matrix S .** This number corresponds to the smallest cardinality of all classes in the respective train sets, i.e. $n = \min_{c \in \mathcal{C}} |c_{\text{train}}|$. For Eurosat it was arbitrarily set to 1000 because no train split was provided.

A.11 Examples of selected descriptions

In this section, we show the obtained descriptions for different datasets in the *json* style below. The ambiguous classes and corresponding selected descriptions of two images for several datasets are shown.

Listing 1: Examples of selected descriptions by our algorithm

```
{
  "image_79": {
    "highway or road": [
      "surrounded by parking lots or roads",
      "parking spaces or driveways",
      "man-made structures like lamps or signs",
      "road markings",
      "vehicles"
    ],
    "brushland or shrubland": [
      "dense vegetation",
      "tree trunks and branches",
      "random patterns",
      "natural curves and lines",
      "randomly distributed shadows"
    ],
    "permanent crop land": [
      "change in crop type or growth stage through the seasons",
      "green color during growing season",
      "texture of crops such as rows of plants or scattered crops",
      "farmland patterns",
      "irregular shapes"
    ]
  },
  "image_13182": {
    "residential buildings or homes or apartments": [
      "uninterrupted spaces",
      "straight rows",
      "man-made structures"
    ],
    "industrial buildings or commercial buildings": [
      "may be clustered together in groups"
    ]
  }
}
```

```

"permanent crop land": [
    "large, rectangular fields",
    "straight rows of crops",
    "irrigation systems",
    "green vegetation",
    "typically have a rectangular or
        square shape"
],
},
"image_1103": {
    "perforated": [
        "Intricate and delicate patterns",
        "repeated floral or geometric design"
        ,
        "Raised ridges on the surface",
        "Uniform pattern of parallel ridges",
        "consistent patterns"
    ],
    "crosshatched": [
        "often darker color",
        "stretchy and flexible",
        "often surrounded by loose debris",
        "often darker coloration",
        "irregular swirls or streaks"
    ],
    "meshed": [
        "fine mesh-like structure",
        "straight lines",
        "sharp lines",
        "continuous curved lines",
        "distinct layers of different colors"
    ],
},
"image_1440": {
    "smeared": [
        "intermingling of colors",
        "consisting of straight lines",
        "uneven distribution of color",
        "seemingly messy look",
        "blurred edges"
    ],
    "stained": [
        "fine, thin strands",
        "stretchy and flexible",
        "Curved teardrop shapes",
        "long and fine strands",
        "Folds of fabric that create a wavy
            pattern"
    ],
    "blotchy": [
        "Intricate and delicate patterns",
        "fine mesh-like structure",
        "repeated floral or geometric design"
        ,
        "Raised ridges on the surface",
        "Uniform pattern of parallel ridges"
    ],
},
"image_4747": {
    "Chestnut sided Warbler": [
        "yellow face",
        "greenish upperparts",
        "white underparts",
        "split white wing bars",
        "white spectacles"
    ]
}

```

```

],
" Nelson Sharp tailed Sparrow": [
    "Bay breast and flanks",
    "black streaking on sides",
    "black face",
    "bold black streaking on sides",
    "black streaking on its back and
        sides"
],
" Bay breasted Warbler": [
    "chestnut-colored flanks",
    "distinctive chestnut-colored patch
        on its flanks",
    "chestnut-colored crown",
    "Black cap",
    "olive-green upperparts"
],
},
"image_3485": {
    "Eastern Towhee": [
        "Bay breast and flanks",
        "black streaking on sides",
        "greenish upperparts",
        "black face",
        "chestnut-colored flanks"
    ],
    "Harris Sparrow": [
        "distinctive chestnut-colored patch
            on its flanks",
        "white underparts",
        "pale underparts",
        "Pale underparts",
        "grayish-brown overall coloration"
    ],
    "Northern Waterthrush": [
        "yellow face",
        "olive-green upperparts",
        "grayish-olive upperparts",
        "white eye ring",
        "small size"
    ],
},
"image_4716": {
    "clematis": [
        "lance-shaped leaves",
        "daisy-like flowers",
        "single row of petals",
        "stem is hairy",
        "colorful flowers, but not bright
            red"
    ],
    "columbine": [
        "cluster of stems",
        "daisy-like flowers with white petals
            and yellow centers",
        "delicate petals",
        "upright, clump-forming habit",
        "pale blue, white, or pink flowers"
    ],
    "balloon flower": [
        "leaves are simple and alternate",
        "cup-shaped flowers",
        "tall stem",
        "solitary stem",
        "umbrella-like leaf structure"
    ]
}

```

```

        ],
        "image_4981": {
            "desert-rose": [
                "cluster of stems",
                "colorful flowers, but not bright red",
                "thick, waxy leaves",
                "typically rosette-forming growth habit",
                "fragrant, delicate, pale pink to deep pink flowers"
            ],
            "frangipani": [
                "lance-shaped leaves",
                "daisy-like flowers with white petals and yellow centers",
                "daisy-like flowers",
                "leaves are simple and alternate",
                "cup-shaped flowers"
            ],
            "mexican petunia": [
                "single row of petals",
                "stem is hairy",
                "delicate petals",
                "tall stem",
                "solitary stem"
            ],
            "image_18780": {
                "ski_slope": [
                    "icy slopes",
                    "ski lifts",
                    "ski slopes",
                    "ski equipment",
                    "ski tracks"
                ],
                "bridge": [
                    "ornamental bridges",
                    "arches or spans for carrying a road or railway",
                    "river or stream",
                    "natural rock formations around the water",
                    "surrounded by walls or embankments"
                ],
                "ski_resort": [
                    "gambrel or gable roof",
                    "snow cover",
                    "covered in snow",
                    "snow-capped roof",
                    "snow-covered roof"
                ],
                "image_100": {
                    "banquet_hall": [
                        "seating arrangement for events",
                        "chairs arranged for dining",
                        "decorative table settings",
                        "place settings on the table",
                        "formal table settings"
                    ],
                    "dining_hall": [
                        "outdoor seating area",
                        "outdoor seating",
                        "outdoor seating"
                    ]
                }
            }
        }
    ]
}

```

```

        ],
        "patio_seating",
        "grilling_area",
        "food served in containers"
    ],
    "ballroom": [
        "dancing",
        "performer on a central stage",
        "vertical sliding movement",
        "skaters wearing figure skates",
        "steps"
    ],
    "image_20": {
        "abyssinian": [
            "almond-shaped eyes",
            "dark, expressive eyes",
            "large eyes",
            "large, expressive eyes",
            "soulful eyes"
        ],
        "bengal": [
            "wrinkled face",
            "curled tail",
            "thick, fluffy coat",
            "high energy level",
            "bushy eyebrows and beard"
        ],
        "egyptian_mau": [
            "a long, thick coat that is usually white with darker markings",
            "a thick, double coat of fur that is black and silver or black and cream in color",
            "blue-grey fur",
            "white markings on the chest, feet, and face",
            "black, fawn, or silver coat"
        ],
        "image_2186": {
            "newfoundland": [
                "black, grey, or brown fur",
                "dark brown or black fur",
                "brindle, black, or blue coat",
                "brindle, fawn, or black coat",
                "black, grey, or brindle"
            ],
            "great_pyrenees": [
                "a long, thick coat that is usually white with darker markings",
                "a large, white, fluffy dog",
                "a dense, wavy coat that is wheaten in color",
                "a white, fluffy coat",
                "white paws"
            ],
            "english_cocker_spaniel": [
                "droopy ears",
                "wet nose",
                "webbed feet",
                "small ears",
                "long, droopy ears"
            ]
        }
    }
}

```

A.12 Example of a description pool P

In this section, we show parts of the LLM assignments of the places dataset. Dissolving the LLM assignments and collecting the classname-less descriptions in a global pool yields the pool P . It is such a pool P that our Algorithm 1 selects from.

```
{  
  "index_to_descriptions": {  
    "0": [  
      "a repeating pattern of light and dark  
      bands",  
      "the bands are of different widths",  
      "the bands may be of different colors",  
      "the bands may be curved or straight",  
      "the bands may be parallel or  
      intersecting"  
    ],  
    "1": [  
      "an uneven or mottled surface",  
      "a variety of colors or shades",  
      "a raised or bumpy texture",  
      "a matte finish"  
    ],  
    "2": [  
      "three or more strands of material woven  
      together",  
      "a tight, interlocking pattern"  
    ],  
    "3": [  
      "small, round, and raised bumps",  
      "a smooth or glossy surface",  
      "a three-dimensional appearance",  
      "a light-reflecting quality"  
    ],  
    "4": [  
      "an uneven surface",  
      "raised or indented areas",  
      "a rough or bumpy feel"  
    ],  
    "5": [  
      "a repeating pattern of squares or  
      rectangles",  
      "alternating light and dark colors",  
      "sharp, defined lines between the squares  
      or rectangles"  
    ],  
    "6": [  
      "a web-like pattern",  
      "made of thin, silky strands",  
      "often found in dark, damp places",  
      "can be sticky to the touch",  
      "can be difficult to remove once  
      entangled"  
    ],  
    "7": [  
      "a surface with cracks",  
      "the cracks may be straight or curved",  
      "the cracks may be of different sizes",  
      "the cracks may be close together or far  
      apart",  
      "the cracks may be deep or shallow",  
      "the cracks may be filled with dirt or  
      debris"  
    ]  
  }  
}
```

```
],
"8": [
  "a series of parallel lines that
  intersect to form a grid",
  "the lines may be of different
  thicknesses",
  "the lines may be of different colors",
  "the texture may be regular or irregular"
  ,
  "the texture may be applied to a surface
  or object"
],
"9": [
  "a repeating pattern of shapes",
  "sharp edges",
  "a glossy or shiny surface",
  "a transparent or translucent appearance"
  ,
  "a three-dimensional structure"
],
"10": [
  "a series of small, round dots",
  "evenly spaced",
  "can be of any color",
  "may be on a background of any color",
  "may be in a regular or irregular pattern"
  "
],
.
.
.
.

},
"index_to_classname": {
  "0": "banded",
  "1": "blotchy",
  "2": "braided",
  "3": "bubbly",
  "4": "bumpy",
  "5": "chequered",
  "6": "cobwebbed",
  "7": "cracked",
  "8": "crosshatched",
  "9": "crystalline",
  "10": "dotted",
  "11": "fibrous",
  .
  .
  .
}
}
```